



## Thermodynamic assessment of ZnO–SiO<sub>2</sub> system

Iikka ISOMÄKI<sup>1</sup>, Rui ZHANG<sup>2</sup>, Long-gong XIA<sup>3</sup>, Niko HELLENSTEN<sup>1</sup>, Pekka A. TASKINEN<sup>1</sup>

1. Thermodynamics and Modelling Research Group, Department of Materials Science and Engineering, School of Chemical Technology, Aalto University, P. O. Box 16200, FI-00076 Aalto, Finland;
2. Department of Materials Science, Royal Institute of Technology, Stockholm 11428, Sweden;
3. School of Metallurgy and Environment, Central South University, Changsha 410083, China

Received 23 October 2017; accepted 10 May 2018

**Abstract:** ZnO-containing slags are common in pyrometallurgical processing of the base metals and steel. This caused the interest to the thermodynamics of the ZnO–SiO<sub>2</sub> system. A complete literature survey, critical evaluation of the available experimental data and a thermodynamic optimization of the phase equilibria and thermodynamic properties of the system ZnO–SiO<sub>2</sub> at 1.013×10<sup>5</sup> Pa are presented. The molten oxide was described as an associate solution. The properties of liquid were reassessed and enthalpy term of the Gibbs energy of solid Zn<sub>2</sub>SiO<sub>4</sub> was re-fitted to be compatible with the new data in the willemite primary phase field. The thermodynamic data set agrees well with the recent experimental observations. It can be used for predicting, e.g., the thermodynamic properties and the domains of the phase diagram, like critical point of the liquid miscibility gap, with a better accuracy than using the previous assessments. A set of optimized model parameters were obtained, reproducing the reliable thermodynamic and phase equilibrium data within their experimental errors from 298 K to liquidus temperatures, over the entire composition range. The created database can be used in a Gibbs energy minimization software to calculate the thermodynamic properties and the phase diagram sections of interest.

**Key words:** thermodynamic assessment; ZnO–SiO<sub>2</sub> system; thermodynamic properties; phase diagram

### 1 Introduction

Considerable interest has been directed towards the development of advanced materials based on zinc oxide over the years [1–4]. Zinc silicate is one of the most promising new material systems due to its unique electrical and physical properties [5–7]. Zinc is also a common impurity element in copper ores and thus its detailed chemistry in silicate systems is of interest when smelting complex raw materials [8]. The purpose of this paper is to present a critical review of the available experimental thermodynamic and phase equilibrium data for the binary ZnO–SiO<sub>2</sub> system, and to obtain an updated set of self-consistent thermodynamic model parameters to describe the system properties.

The binary ZnO–SiO<sub>2</sub> system has been experimentally studied [9–15] and thermodynamically assessed by a few researchers [16,17]. ZnO–SiO<sub>2</sub> was studied, because it is a part of PbO–ZnO–FeO–Fe<sub>2</sub>O<sub>3</sub>–CaO–SiO<sub>2</sub> zinc/lead smelting slags and sinter [15]. ZnO-

containing slags are also commonly formed in the pyrometallurgical processing of zinc, lead, copper and steel [15].

BUNTING [9] measured the ZnO–SiO<sub>2</sub> phase diagram features using an equilibration-quenching-optical microscopy analysis technique and found a large liquid immiscibility region on the SiO<sub>2</sub>-rich side at elevated temperatures, one compound (willemite or zinc orthosilicate Zn<sub>2</sub>SiO<sub>4</sub>), and two eutectic reactions ( $L \rightarrow \text{SiO}_2 + \text{Zn}_2\text{SiO}_4$  and  $L \rightarrow \text{ZnO} + \text{Zn}_2\text{SiO}_4$ ). A monotectic equilibrium of two immiscible liquids in equilibrium with cristobalite was reported to extend mole fraction of ZnO from 0.02 to 0.35, and the compound to melt congruently at (1785±3) K. Eutectic points were determined to be 1705 K and mole fraction of ZnO of 0.491 on SiO<sub>2</sub> saturation side, and 1780 K and mole fraction of ZnO of 0.775 on ZnO saturation side. However, the compositions of the liquidus line in the paper of BUNTING [9] were reported as the initial compositions of the samples, prior to equilibration. Impurities in the starting materials as well as evaporation

of ZnO at elevated temperatures [18] did bring about unpredictable errors to his results.

WILLIAMSON and GLASSER [10], and WEBER et al [11,12] re-investigated experimentally the ZnO–SiO<sub>2</sub> system. Their data agreed well with the findings of BUNTING [9] at the eutectic point in the silica-rich region. The eutectic point between Zn<sub>2</sub>SiO<sub>4</sub> and ZnO, however, was much lower than the value proposed by BUNTING [9], and the location of the liquidus was not well explained in their studies. RINGWOOD and MAJOR [19], SYONO et al [20], AKAOGI et al [21] and LIU et al [22] used high-temperature X-ray techniques for measuring the (*P*, *T*)-phase diagrams of zinc silicates.

REYES and GASKELL [13] measured the activity of ZnO in the ZnO–SiO<sub>2</sub> melts at 1833 K using a transpiration technique with CO–CO<sub>2</sub> mixture as the carrier gas. The measured Gibbs energies of formation of ZnO–SiO<sub>2</sub> melts were significantly more negative than the estimated value [9,11,12], indicating that ZnO is a relatively basic oxide. ITOH and AZAKAMI [23] conducted EMF measurements in the solid mixtures of the system using oxygen concentration cells. Calorimetric measurements are also available on the zinc orthosilicate–metasilicate transition pressure [24].

BJÖRKMAN [16] initially assessed the ZnO–SiO<sub>2</sub> system by treating the liquid oxide mixture as an ideal solution, but he considered the formation of Zn<sub>2</sub>SiO<sub>4</sub> as an associated species, which reduced the concentration and thus the activity of “free” ZnO. The calculated phase relations as well as the activity of ZnO were found to be in a good agreement with the available data. JAK et al [17,25] optimized the ZnO–SiO<sub>2</sub> system by employing the quasi-chemical model for the liquid silicate and least-squares optimization module of the F\*A\*C\*T software package [26]. The thermodynamic properties of SiO<sub>2</sub> were taken from the F\*A\*C\*T database, and the properties of ZnO from BARIN [27]. The thermodynamic information about Zn<sub>2</sub>SiO<sub>4</sub> was insufficient in Refs. [28–32]. Therefore, JAK et al [17] adopted the standard entropy of Zn<sub>2</sub>SiO<sub>4</sub> from the compilation of BARIN [27], and optimized the other thermodynamic properties of Zn<sub>2</sub>SiO<sub>4</sub>. The experimental phase diagram points used in the optimization [9–12] were reproduced well by the assessed parameters in their study.

The development of advanced experimental apparatus and analytical techniques makes it possible for the researchers to control the experimental conditions and achieve results efficiently and in more reliable way. HANSSON et al [14] experimentally studied the phase equilibria and liquidus temperatures of the ZnO–SiO<sub>2</sub> system using an equilibration-quenching-EPMA (electron probe X-ray microanalysis) technique [33].

Two binary eutectics points involving congruently melting willemite (m.p. (1785±3) K) were ascertained to be (1721±5) K and mole fraction of ZnO of 0.52±0.01, and (1775±5) K and mole fraction of ZnO of 0.71±0.01, respectively. XIA et al [15] studied the ZnO–SiO<sub>2</sub> system using an equilibration and quenching technique in a wide temperature range from 1703 to 1963 K. Their results obtained by EPMA confirmed the findings reported by HANSSON et al [14] and expanded the experimental data range.

A few experimental attempts have also been made on re-determining the thermodynamic properties of Zn<sub>2</sub>SiO<sub>4</sub> [23,24,34]. Also, a first principles study about the stability of zinc silicates in high pressures has been carried out [35]. BEKTURGANOV et al [36] calculated the low-temperature *c<sub>p</sub>* function (*c<sub>p</sub>* is the specific heat capacity) of willemite by ab initio techniques.

## 2 Critical review of experimental data

The experimental phase diagram measurements of the ZnO–SiO<sub>2</sub> system and the available thermodynamic data of Zn<sub>2</sub>SiO<sub>4</sub> from the literature were compiled and evaluated critically. The recent phase diagram studies [14,15] deviate systematically from the older observations [9–12] which involve systematical errors and uncertainties. An additional problem with the experimental phase diagram and liquidus data is that the measurements have been made at relatively low temperatures. No experimental data about the critical point of the molten-state miscibility gap at silica-rich compositions could be found. The zinc oxide activity data obtained by REYES and GASKELL [13] using vapor pressure transpiration measurements seem to be too low at small zinc oxide concentrations, i.e., in the silica-rich compositions obviously due to systematic errors in their experimental method. The transpiration method may have faced problems in attaining equilibrium between the flowing CO–CO<sub>2</sub> gas and molten sample, due to the small reaction interface. Due to large differences between the recent experimental data by HANSSON et al [14] and XIA et al [15] and the computational phase diagrams from the 20th century, the system was found to require reassessment.

## 3 Thermodynamic modelling

The thermodynamic modelling and the model parameter optimization were carried out using the Calphad technique in the Thermo-Calc software environment [37].

### 3.1 Unary phases

The Gibbs energy of a component *i* in phase *φ*,  ${}^{\ominus}G_i^{\phi} = G_i^{\phi}(T) - H_i^{\text{SER}}$  (*i*=ZnO and SiO<sub>2</sub>) was expressed

by the following equation:

$${}^{\ominus}G_i^{\phi} = a + bT + cT \ln T + dT^2 + eT^{-1} + fT^3 + gT^7 + hT^{-9} \quad (1)$$

where  $H_i^{\text{SER}}$  is the sum of enthalpies of the elements at 298.15 K and  $1.013 \times 10^5$  Pa in their stable states (stable element reference, denoted as SER);  $T$  is the thermodynamic temperature (K) and parameters  $a-h$  are substance specific coefficients. In this work, the Gibbs energy functions used for pure ZnO are consistent with MTDATA [38] and the Mtox oxide database [39]. The Gibbs energy expression for pure SiO<sub>2</sub> was taken from SGTE\_SUB database by MTDATA [40].

### 3.2 Solution phases

An associate solution model was employed to describe the liquid oxide phase [41] which was assumed to consist of three species: ZnO, Zn<sub>2</sub>SiO<sub>4</sub> and SiO<sub>2</sub>. The molar Gibbs energy of liquid oxide solution can thus be expressed as follows:

$$\begin{aligned} G_m^{\text{Liq}} - H^{\text{SER}} = & y_{\text{ZnO}} {}^{\ominus}G_{\text{ZnO}}^{\text{Liq}} + y_{\text{SiO}_2} {}^{\ominus}G_{\text{SiO}_2}^{\text{Liq}} + \\ & y_{\text{Zn}_2\text{SiO}_4} {}^{\ominus}G_{\text{Zn}_2\text{SiO}_4}^{\text{Liq}} + RT(y_{\text{ZnO}} \ln y_{\text{ZnO}} + \\ & y_{\text{SiO}_2} \ln y_{\text{SiO}_2} + y_{\text{Zn}_2\text{SiO}_4} \ln y_{\text{Zn}_2\text{SiO}_4}) + {}^{\text{E}}G_m \end{aligned} \quad (2)$$

where  $y$  represents the mole fraction of an associate ZnO, SiO<sub>2</sub> and Zn<sub>2</sub>SiO<sub>4</sub> in the liquid oxide solution. The symbol  $y$  was used for the associate concentrations in order to distinguish from the macroscopic component concentrations in figures denoted as  $x$ . The Gibbs energy of molten zinc orthosilicate associate  ${}^{\ominus}G_{\text{Zn}_2\text{SiO}_4}^{\text{Liq}}$  was described as

$${}^{\ominus}G_{\text{Zn}_2\text{SiO}_4}^{\text{Liq}} = 2G_{\text{ZnO}}^{\text{Liq}} + G_{\text{SiO}_2}^{\text{Liq}} + a + bT + cT \ln T \quad (3)$$

where  ${}^{\ominus}G_{\text{ZnO}}^{\text{Liq}}$  and  ${}^{\ominus}G_{\text{SiO}_2}^{\text{Liq}}$  are Gibbs energies of liquid ZnO and SiO<sub>2</sub>, respectively, and  $a$  and  $b$  are the enthalpy and entropy of formation of zinc orthosilicate (Zn<sub>2</sub>SiO<sub>4</sub>) associate, respectively.

In Eq. (2),  ${}^{\text{E}}G_m$  is excess Gibbs energy of the liquid oxide phase, which was described by Redlich–Kister polynomials [42] as

$$\begin{aligned} {}^{\text{E}}G_m = & y_{\text{ZnO}} y_{\text{SiO}_2} [{}^0L_{\text{ZnO},\text{SiO}_2} + {}^1L_{\text{ZnO},\text{SiO}_2} (y_{\text{ZnO}} - y_{\text{SiO}_2})] + \\ & y_{\text{ZnO}} y_{\text{Zn}_2\text{SiO}_4} [{}^0L_{\text{ZnO},\text{Zn}_2\text{SiO}_4} + {}^1L_{\text{ZnO},\text{Zn}_2\text{SiO}_4} (y_{\text{ZnO}} - \\ & y_{\text{Zn}_2\text{SiO}_4})] + y_{\text{SiO}_2} y_{\text{Zn}_2\text{SiO}_4} [{}^0L_{\text{SiO}_2,\text{Zn}_2\text{SiO}_4} + \\ & {}^1L_{\text{SiO}_2,\text{Zn}_2\text{SiO}_4} (y_{\text{SiO}_2} - y_{\text{Zn}_2\text{SiO}_4}) + \\ & {}^2L_{\text{SiO}_2,\text{Zn}_2\text{SiO}_4} (y_{\text{SiO}_2} - y_{\text{Zn}_2\text{SiO}_4})^2] \end{aligned} \quad (4)$$

where  ${}^lL_{\text{ZnO},\text{SiO}_2}$ ,  ${}^lL_{\text{ZnO},\text{Zn}_2\text{SiO}_4}$  and  ${}^lL_{\text{SiO}_2,\text{Zn}_2\text{SiO}_4}$  ( $l=0, 1, 2$ ) are the interaction parameters between different species to be optimized in the present work. No ternary parameters were needed. A general temperature dependent form of the interaction parameters  ${}^lL_{i,j} = c + dT$  was used.

It should be pointed out on the basis of the literature review summarized above that no experimental data could be found on the mutual solubilities between the solid ZnO (wurtzite) and SiO<sub>2</sub> (tridymite, cristobalite) phases. Therefore, in the present work, the terminal (solid) solutions (ZnO-based and SiO<sub>2</sub>-based solutions) in the ZnO–SiO<sub>2</sub> system have been treated as pure oxides in the parameter optimization.

### 3.3 Compounds

Based on the literature review, a solid orthosilicate compound willemite (Zn<sub>2</sub>SiO<sub>4</sub>) has been confirmed to exist in the ZnO–SiO<sub>2</sub> system at ambient pressure [24]. The molar Gibbs energy function of this olivine type stoichiometric compound [20] was expressed as

$${}^{\ominus}G_{\text{Zn}_2\text{SiO}_4} - 2H_{\text{Zn}}^{\text{SER}} - H_{\text{Si}}^{\text{SER}} - 4H_0^{\text{SER}} = A + BT + CT \ln T + DT^2 + FT^{-1} \quad (5)$$

where  $A-F$  are coefficients specific to Zn<sub>2</sub>SiO<sub>4</sub>. The thermodynamic coefficients retrieved from the Mtox oxide database [39] were employed to initially describe the properties of solid and liquid Zn<sub>2</sub>SiO<sub>4</sub>. The zinc metasilicate ZnSiO<sub>3</sub> crystallizing as pyroxene or ilmenite structure is stable at elevated pressures only [20,24,43] and thus it was not included in the present optimization.

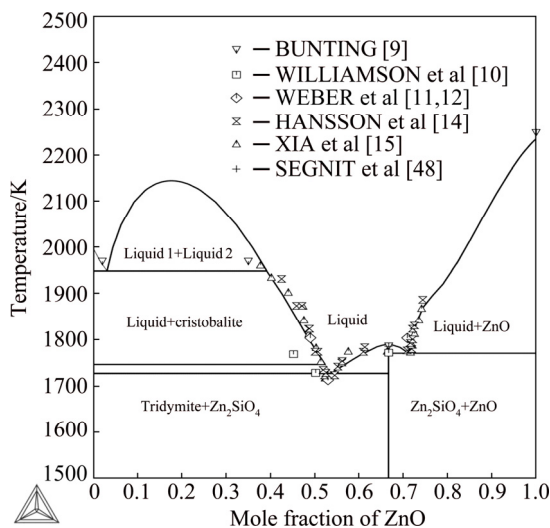
The optimization of the thermodynamic parameters was performed manually using the CALPHAD technique [44] and the Thermo-Calc 2016a and 2016b [37] software package. A step-by-step optimization procedure was adopted and the data of new experiments [15] as well as selected literature data were employed. Firstly, the binary parameters  ${}^lL_{\text{SiO}_2,\text{Zn}_2\text{SiO}_4}$  and  ${}^lL_{\text{ZnO},\text{Zn}_2\text{SiO}_4}$  were evaluated. After achieving a good fit with the experimental data for the liquid oxide phase, the enthalpy parameter for solid Zn<sub>2</sub>SiO<sub>4</sub> (see Eq. (5)), was calculated. Only the enthalpy of solid willemite was reassessed, for adjusting the liquidus line within the willemite primary phase field according to the recent liquidus measurements [14,15] and the melting point of willemite. The specific heat capacity parameters were taken from Mtox database [39] as such.

## 4 Results and discussion

The thermodynamic assessment of the ZnO–SiO<sub>2</sub> system was conducted with Parrot starting from zero; however, the parameters for liquid  $L_{\text{ZnO},\text{SiO}_2}^0$  and  $L_{\text{ZnO},\text{SiO}_2}^1$  from MTDATA were used as such. The system was treated as a true binary ZnO–SiO<sub>2</sub> system, even though it is really a quasi-binary section of the ternary Si–O–Zn. In order to maintain compatibility with the Mtox database, the liquid oxide phase was modelled with species ZnO, SiO<sub>2</sub> and Zn<sub>2</sub>SiO<sub>4</sub>, which is a flexible

model for liquid multicomponent silicates [45] compared to ionic liquid model [41], and can reproduce properties of acidic and basic slags with a single parameter set. No adjustments to the primary data were made and they were taken from the original literature sources with appropriate inaccuracies.

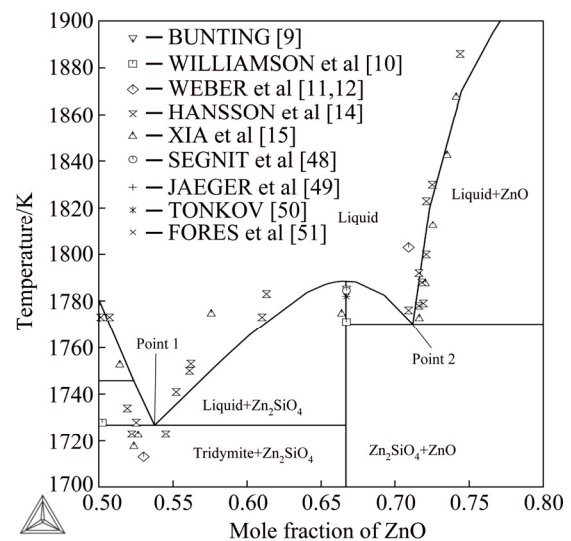
Figure 1 shows the calculated phase diagram for the ZnO–SiO<sub>2</sub> system. The experimental points reproduced in the graph were taken from WILLIAMSON and GLASSER [10], WEBER and GRAUER-CARSTENSEN [11,12], HANSSON et al [14], XIA et al [15]. There are no experimental data available concerning the critical point or tie-lines of the silica-rich miscibility gap, except the monotectic equilibrium. Monotectic temperature according to BUNTING [9] is 1968 K. The calculated monotectic temperature of this work is 1947 K. The resulting critical temperature is 2145 K and its composition  $x_{\text{ZnO}}=0.176$ . The miscibility gap was assessed according to the existing data at much lower temperatures than the critical point. The liquidus curve on the ZnO-rich side is S-shaped, suggesting that there is a metastable miscibility gap [46]. There is a possible submerged metastable miscibility gap with a critical temperature just below the inflection point on the liquidus curve. Often, the immiscibility domain is entirely metastable and is not present on the equilibrium diagram [47].



**Fig. 1** Assessed binary phase diagram of SiO<sub>2</sub>–ZnO with experimental data on liquidus lines superimposed

Figure 2 shows a magnified phase diagram section around the willemite composition and its congruent melting point. The assessed melting point of willemite is 1515.5 °C (1788.5 K) and the experimental values of BUNTING [9], and SEGNET and HOLLAND [48] are 1785 K and 1784.5 K, respectively. The calculated silica-rich eutectic point 1 is located at  $x_{\text{ZnO}}=0.537$  and  $T=1727$  K. The experimental values by XIA et al [15] are

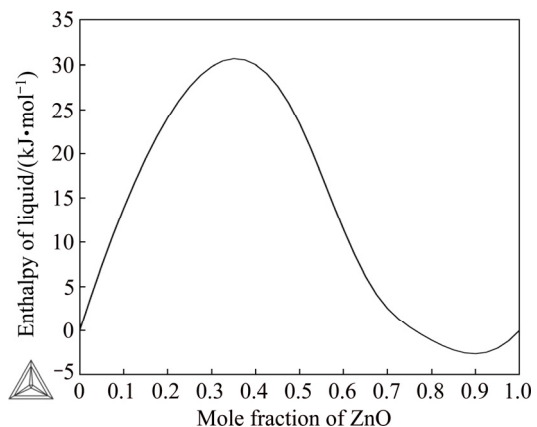
$x_{\text{ZnO}}=0.52$  and  $T=1718$  K. The values obtained by HANSSON et al [14] are  $x_{\text{ZnO}}=0.519$  and  $T=1734$  K. The obtained fit is thus good between the experimental and assessed phase diagram values. The calculated zinc-oxide-rich eutectic point 2 is located at  $x_{\text{ZnO}}=0.711$  and  $T=1770$  K. XIA et al [15] obtained the values of  $x_{\text{ZnO}}=0.716$  and  $T=1773$  K. HANSSON et al [14] reported the values  $x_{\text{ZnO}}=0.72$  and  $T=1779$  K. The obtained agreement of the assessed value with the second eutectic point is very good, and the experimental values of HANSSON et al [14] and XIA et al [15] are reproduced well by the optimized solution properties.



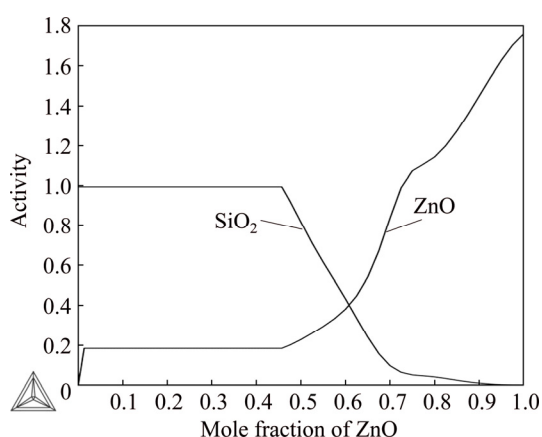
**Fig. 2** Detail of assessed binary phase diagram around willemite and Zn<sub>2</sub>SiO<sub>4</sub> primary phase field

Figure 3 shows the calculated liquid oxide enthalpy plot as a function of composition at 2400 K. The curve obtained is compatible with the formation of miscibility gap in silica-rich compositions. No experimental data were available for comparison of the mixing enthalpy.

Figure 4 shows the assessed activities of ZnO and SiO<sub>2</sub> as a function of ZnO mole fraction at 1833 K. The standard states used in the graph were pure, solid ZnO(s) and pure liquid SiO<sub>2</sub>(l). Figure 5 shows the activities of



**Fig. 3** Assessed enthalpy of mixing of liquid for ZnO–SiO<sub>2</sub> solution at 2400 K (standard states ZnO(l) and SiO<sub>2</sub>(l))



**Fig. 4** Assessed activities of ZnO and SiO<sub>2</sub> in ZnO–SiO<sub>2</sub> system at 1833 K (standard states: ZnO(s) and SiO<sub>2</sub>(l))

ZnO and SiO<sub>2</sub> as a function of zinc oxide mole fraction at 1833 K. Standard states were solid ZnO and cristobalite for SiO<sub>2</sub>. The graph indicates that the ZnO activity values of REYES and GASKELL [13] measured at 1833 K were much too low in the low ZnO concentration region. When system was assessed according to the existing literature data, the ZnO activity data of REYES and GASKELL [13] seem to be too low compared to calculated data. It seems to be incorrect if the other literature data are correct. In their transpiration method, systematic problems of attaining equilibrium between the gas flow and slag sample may have occurred due to the small reaction interface and open design of the cell.

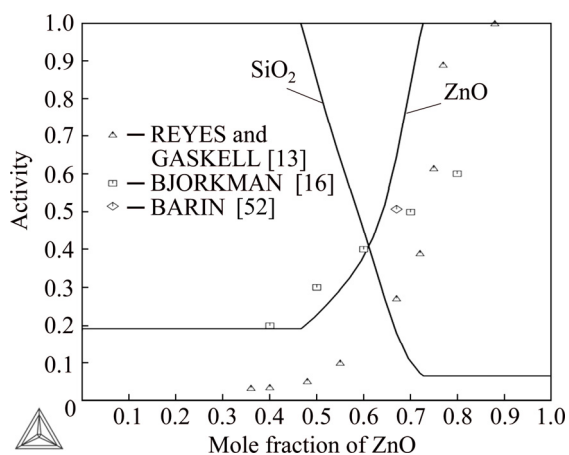
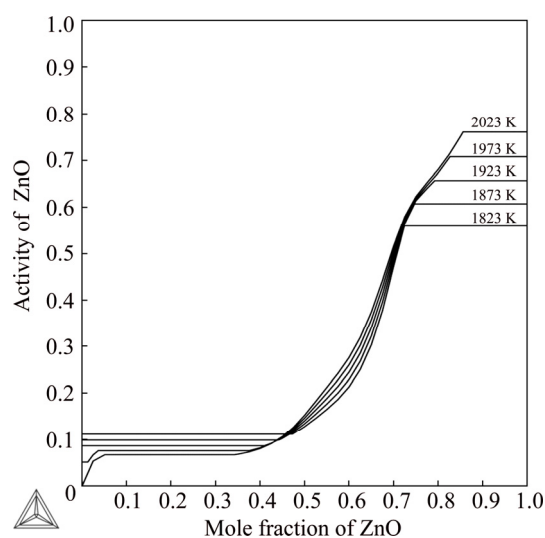


**Fig. 5** Assessed activities of ZnO and SiO<sub>2</sub> in ZnO–SiO<sub>2</sub> system at 1833 K with literature data (standard states: ZnO(s) and SiO<sub>2</sub>(s, cristobalite))

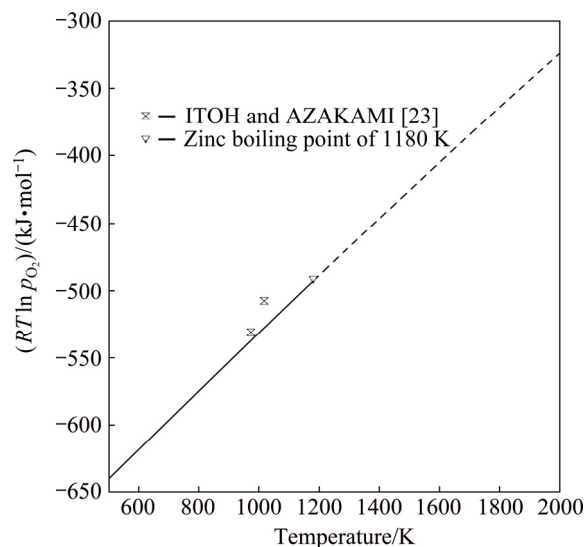
The first three points of BJÖRKMAN [16] agree well with the calculated curve of this study, but his two last points are not so well. BARIN's data [49] were from 1773 K, because at 1833 K willemite is molten. Two experimental points by ITOH and AZAKAMI [23] at 973 and 1073 K agree well with the assessed ZnO activity values of this study.

Figure 6 displays the assessed activity plots of ZnO, with liquid ZnO as the standard state, as a function of composition of ZnO at five temperatures from 1823 to 2023 K with steps of 50 K. The previously assessed values by JAK et al [17] are in good agreement with this study. When the calculated activities of ZnO at 973 and 1073 K at silica saturation according to this work were compared with the experimental values of ITOH and AZAKAMI [23], it was found that the values are well in line with each other. The data were not used in the assessment. The EMF data by ITOH and AZAKAMI [23] show a slightly more negative enthalpy of formation of Zn<sub>2</sub>SiO<sub>4</sub> from the component oxides compared with those obtained by the other authors [29,31,32].

The solid line in Fig. 7 shows the assessed  $RT \ln p_{O_2}$  for the equilibrium reaction (6) between willemite,

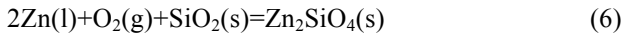


**Fig. 6** Assessed activities of ZnO in ZnO–SiO<sub>2</sub> system from 1823 to 2023 K at 50 K interval (standard state: ZnO(s))



**Fig. 7** Oxygen potential of Zn–SiO<sub>2</sub>–Zn<sub>2</sub>SiO<sub>4</sub> equilibrium according to EMF data by ITOH and AZAKAMI [23] and present assessment (—) and gaseous zinc (----) (standard states: Zn(l), SiO<sub>2</sub>(s), Zn<sub>2</sub>SiO<sub>4</sub>(s))

silica and liquid zinc with pure gaseous oxygen ( $1.013 \times 10^5$  Pa) as standard state:



The dashed line in Fig. 7 shows the area where zinc is gaseous. ITOH and AZAKAMI [23] measured the partial pressures of oxygen for Eq. (6) by an EMF technique in the temperature range from 973 to 1073 K. Their experimental results agree well with the calculated values of this study. Figure 7 represents a straightforward validation for the current assessed data of the ZnO–SiO<sub>2</sub> system, as the experimental values by ITOH and AZAKAMI [23] were not used as experimental points in the parameter optimization.

Table 1 presents the assessed thermodynamic parameters for the liquid phase and Gibbs energy of solid willemite obtained in this study. Table 2 shows the available experimental literature data for the Gibbs energy of formation of solid Zn<sub>2</sub>SiO<sub>4</sub>.

When the results from this work were compared with the available literature data, it was found that the formation enthalpy of Zn<sub>2</sub>SiO<sub>4</sub> obtained at 298 K is near the calorimetric values of KING [28] and TODD [30]. The enthalpy value is almost exactly the same as adopted by BARIN [27].

When the obtained the formation entropy at 298 K is compared to the experimental value of TODD [30], it can be found that results are close to each other. This

**Table 1** Assessed model parameters of ZnO–SiO<sub>2</sub> system obtained in this study

Material	Model parameter
	${}^0L_{\text{ZnO,SiO}_2} = 8183.41521$ , ${}^1L_{\text{ZnO,SiO}_2} = 70897.9728$
Liquid oxide	${}^0L_{\text{SiO}_2,\text{Zn}_2\text{SiO}_4} = 249919.8 - 138.930466T$ , ${}^1L_{\text{SiO}_2,\text{Zn}_2\text{SiO}_4} = 55025.0172 - 16.50422T$ , ${}^2L_{\text{SiO}_2,\text{Zn}_2\text{SiO}_4} = 35001.1539$ ${}^0L_{\text{Zn}_2\text{SiO}_4,\text{ZnO}} = 9999 - 4.25T$ , ${}^1L_{\text{Zn}_2\text{SiO}_4,\text{ZnO}} = -13920 - 3.31T$
Willemite Zn <sub>2</sub> SiO <sub>4</sub> (s)	${}^0G_{\text{Zn}_2\text{SiO}_4} - 2H_{\text{Zn}}^{\text{SER}} - H_{\text{Si}}^{\text{SER}} - 4H_0^{\text{SER}} = -1700400 + 867.065702672T - 144.89T \ln T - 0.01847T^2 + 1514500T^{-1}$
Zn <sub>2</sub> SiO <sub>4</sub> (l)	${}^0G_{\text{Zn}_2\text{SiO}_4} - 2H_{\text{Zn}}^{\text{SER}} - H_{\text{Si}}^{\text{SER}} - 4H_0^{\text{SER}} = -1666364.73 + 1347.6291T - 215 \ln T$

**Table 2** Thermodynamic parameters of formation of solid Zn<sub>2</sub>SiO<sub>4</sub> by different experimental reactions and authors

Reaction	Temperature/K	$\Delta_r H/$ (kJ·mol <sup>-1</sup> )	$\Delta_r S/$ (J·mol <sup>-1</sup> ·K <sup>-1</sup> )	Ref.
Zn <sub>2</sub> SiO <sub>4</sub> +2CO(g)=2Zn(g)+2CO <sub>2</sub> (g)+SiO <sub>2</sub> (s)	1423–1573	491	-273	[34]
2Zn(g)+Si+2O <sub>2</sub> (g)=Zn <sub>2</sub> SiO <sub>4</sub>	1423–1573	-1951	-613	[34]
Zn <sub>2</sub> SiO <sub>4</sub> +2H <sub>2</sub> (g)=2Zn(g)+2H <sub>2</sub> O(g)+SiO <sub>2</sub> (s)	1073–1275	495.3856	321.2057	[29]
2ZnO+SiO <sub>2</sub> =Zn <sub>2</sub> SiO <sub>4</sub>	1073–1275	-29.82774	-0.96232	[29]
2ZnO+SiO <sub>2</sub> =Zn <sub>2</sub> SiO <sub>4</sub>	900–1100	-758.470	-233.85	[23]
2ZnO+SiO <sub>2</sub> =Zn <sub>2</sub> SiO <sub>4</sub>	973–1073	-46.590	-16.79	[23]
2ZnO+SiO <sub>2</sub> =Zn <sub>2</sub> SiO <sub>4</sub>	953–1273	-34.6854	-5.8576	[32]
	298	-29.288		
	965	-32.6352		
2ZnO+SiO <sub>2</sub> =Zn <sub>2</sub> SiO <sub>4</sub>	965	-32.7607	-3.7656	[31]
	1000			
	1173	-29.7064		
2Zn+Si+2O <sub>2</sub> (g)=Zn <sub>2</sub> SiO <sub>4</sub>	298	-1584.481	n.a.	[28]
2ZnO+SiO <sub>2</sub> =Zn <sub>2</sub> SiO <sub>4</sub>	298	-29.2462		[28]
2Zn+Si+2O <sub>2</sub> (g)=Zn <sub>2</sub> SiO <sub>4</sub>	298	-1584.481	-380.744	[30]
2ZnO+SiO <sub>2</sub> =Zn <sub>2</sub> SiO <sub>4</sub>	298	-29.2462	2.092	[30]
2Zn+Si+2O <sub>2</sub> (g)=Zn <sub>2</sub> SiO <sub>4</sub>	298	-1645.400	-380.97	This work
2ZnO+SiO <sub>2</sub> =Zn <sub>2</sub> SiO <sub>4</sub>	298	-33.780	2.6398	This work
2ZnO+SiO <sub>2</sub> =Zn <sub>2</sub> SiO <sub>4</sub>	298	-32.6352	n.a.	[53]
2Zn(s)+Si+2O <sub>2</sub> (g)=Zn <sub>2</sub> SiO <sub>4</sub>	298	-1644.412	-380.996	[27]
2Zn(s)+Si+2O <sub>2</sub> (g)=Zn <sub>2</sub> SiO <sub>4</sub>	1400	-1866.57	-573.931	[27]
2Zn(g)+Si+2O <sub>2</sub> (g)=Zn <sub>2</sub> SiO <sub>4</sub>	1500	-1861.13	-570.181	[27]

entropy value is almost exactly the same as compiled by BARIN [27].

When results from this work are compared to literature, it was found that the formation enthalpy of  $Zn_2SiO_4$  from oxides at 298 K obtained in this work is near the values obtained by KING [28], TODD [30], NAVROTSKY [31] and KUBASCHEWSKI and ALCOCK [50]. Entropy for formation from oxides at 298 K obtained in this work is close the value given by TODD [30].

When enthalpy values obtained by KITCHENER and IGNATOWICZ [29] for formation of  $Zn_2SiO_4$  from oxides at elevated temperatures are compared with the values obtained by NAVROTSKY [31] and KOZLOVSKA-RÓG and RÓG [32], it was found that they vary from  $-29.3$  to  $-34.7$  kJ/mol. The deviating value by ITOH and AZAKAMI [23] is  $-46.6$  kJ/mol and it was obtained by EMF techniques over a narrow temperature interval. The value of this work at 298 K is  $-33.8$  kJ/mol, which is very good in the range of the experimental literature data.

When entropy values from KITCHENER and IGNATOWICZ [29] for the formation of  $Zn_2SiO_4$  from oxides at elevated temperatures are compared to NAVROTSKY [31] and KOZLOVSKA-RÓG and RÓG [32], it was found that all values are from  $-5.86$  to  $-0.96$  J/(mol·K). ITOH and AZAKAMI [23] obtained a much more negative value of  $-16.79$  J/(mol·K). The value from this work at 298 K is  $2.64$  J/(mol·K) which is near the value of TODD [30] ( $2.09$  J/(mol·K)).

## 5 Conclusions

1) ZnO–SiO<sub>2</sub> containing slags are common in the primary and secondary pyroprocessing of base metals and steel. Therefore, the ZnO–SiO<sub>2</sub> system was reassessed using the description of Mtox oxide database as the starting point. SiO<sub>2</sub> pure substance values were taken from the SGTE SUB pure substance database and those for ZnO from Mtox. The properties of liquid oxide phase were reassessed totally and also the enthalpy term of the Gibbs energy of solid  $Zn_2SiO_4$ . The new thermodynamic modelling agrees well with the recent experimental data and it can be used for predicting, e.g., areas of the phase diagram without experimental points, like the critical point of the liquid miscibility gap, with better accuracy than using the previous assessments.

2) The obtained fit between the recent experimental data and assessed phase boundaries was good. Mixing enthalpies of the liquid oxide phase at 2400 K were calculated and the results seem reasonable, but no experimental observations are available for the validation of the results. Also, the experimental ZnO activity data from the literature were compared with the calculated

results and the agreement was good, except for the vapour pressure measurements by REYES and GASKELL [13]. Their experimental ZnO activities were too low at low ZnO concentrations of the ZnO–SiO<sub>2</sub> system, and the obtained transpiration zinc activity data seem to be fully incompatible with the other observations as well as with the assessed properties of this study. The present assessed activities in the liquid oxide phase at five temperatures are in good agreement with the calculated values from the previous optimization by JAK et al [17].

3) Calculated oxygen chemical potential agrees quite well with that from ITOH and AZAKAMI [23]. The obtained parameter set also contains less terms than the Mtox description, i.e., 7 terms compared to the original 11, with 11 adjustable parameters vs 17.

## Acknowledgments

The authors like to acknowledge the financial support of Tekes, Fimecc Oy (SIMP program), Finnish Metals Producers Fund and CIMO (Centre for International Movement, an agency of Finnish Ministry of Education and Culture).

## References

- [1] ÖZGÜR Ü, ALIVOV Y I, LIU C, TEKE A, RESCHNIKOV M, DOĞAN S, AVRUTIN V C, CHO S J, MORKOC H. A comprehensive review of ZnO materials and devices [J]. *Journal of Applied Physics*, 2005, 98: 041301
- [2] KLINGSHIRN C. ZnO: From basics towards applications [J]. *Physica Status Solidi*, 2007, 244: 3027–3073.
- [3] KUMAR, R, KUMAR G, AL-DOSSARY O, UMAR A. ZnO nanostructured thin films: Depositions, properties and applications—A review [J]. *Materials Express*, 2015, 5: 3–23.
- [4] MA H, WILLIAMS P L, DIAMOND S A. Ecotoxicity of manufactured ZnO nanoparticles—A review [J]. *Environmental Pollution*, 2013, 172: 76–85.
- [5] ISKANDAR F. Nanoparticle processing for optical applications—A review [J]. *Advanced Powder Technology*, 2009, 20: 283–292.
- [6] VIITANEN M M, JANSEN W P, van WELZENIS R G, BRONGERSMA H H, BRANDS D S, POELS E K, BLIEK A. Cu/ZnO and Cu/ZnO/SiO<sub>2</sub> catalysts studied by low-energy ion scattering [J]. *The Journal of Physical Chemistry B*, 1999, 103: 6015–6029.
- [7] GAO G, REIBSTEIN S, PENG M, WONDRACZEK L. Tunable dual-mode photoluminescence from nanocrystalline Eu-doped Li<sub>2</sub>ZnSiO<sub>4</sub> glass ceramic phosphors [J]. *Journal of Materials Chemistry*, 2011, 21: 3156–3161.
- [8] HABASHI F. Recent trends in extractive metallurgy [J]. *Journal of Mining and Metallurgy B*, 2009, 45: 1–13.
- [9] BUNTING E N. Phase equilibria in the system SiO<sub>2</sub>–ZnO [J]. *Journal of Research National Bureau of Standards*, 1930, 13: 131–136.
- [10] WILLIAMSON J, GLASSER F P. Crystallisation of zinc silicate liquids and glasses [J]. *Physics and Chemistry of Glasses*, 1964, 5: 52–59.
- [11] WEBER L, GRAUER-CARSTENSEN E. The solidification

- behaviour of melts in the system  $Zn_2SiO_4$ – $Mg_2SiO_4$  [J]. *Journal of Materials Science*, 1977, 12: 1988–1993.
- [12] WEBER L, OSWALD H R. Investigation of phase intergrowth morphologies in the system  $Zn_2SiO_4$ – $SiO_2$  by photo-emission electron microscopy [J]. *Journal of Materials Science*, 1975, 10: 973–982.
- [13] REYES R A, GASKELL D R. Thermodynamic activity of ZnO in silicate melts [J]. *Metallurgical Transactions B*, 1983, 14B: 725–731.
- [14] HANSSON R, ZHAO B J, HAYES P C, JAK E A. A reinvestigation of phase equilibria in the system  $Al_2O_3$ – $SiO_2$ – $ZnO$  [J]. *Metallurgical and Materials Transactions B*, 2005, 36: 187–193.
- [15] XIA L, LIU Z, TASKINEN P A. Experimental determination of the liquidus temperatures of the binary ( $SiO_2$ – $ZnO$ ) system in equilibrium with air [J]. *Journal of the European Ceramic Society*, 2015, 35: 4005–4010.
- [16] BJÖRKMANN B. An assessment of Cu, Ni, and Zn silicate systems: I. The binary systems  $CuO_{0.5}$ – $SiO_2$ ,  $NiO$ – $SiO_2$  and  $ZnO$ – $SiO_2$  [J]. *Scandinavian Journal of Metallurgy*, 1986, 15: 185–190.
- [17] JAK E, DEKTEROV S, WU P, HAYES P C, PELTON A. Thermodynamic optimization of the systems  $PbO$ – $SiO_2$ ,  $PbO$ – $ZnO$ ,  $ZnO$ – $SiO_2$  and  $PbO$ – $ZnO$ – $SiO_2$  [J]. *Metallurgical and Materials Transactions B*, 1997, 28: 1011–1018.
- [18] WRIEDT H A. The O–Zn (oxygen–zinc) system [J]. *Bulletin of Alloy Phase Diagrams*, 1987, 8: 166–176.
- [19] RINGWOOD A E, MAJOR A. High pressure transformations in zinc germanates and silicates [J]. *Nature*, 1967, 215: 1367–1368.
- [20] SYONO Y, AKIMOTO S, MATSUI Y. High pressure transformations in zinc silicates [J]. *Journal of Solid State Chemistry*, 1971, 3: 369–380.
- [21] AKAOGI M, YUSA H, ITO E, YAGI T, SUIITO K, IYAMA J T. The  $ZnSiO_3$  clinopyroxene–ilmenite transition: Heat capacity, enthalpy of transition, and phase equilibria [J]. *Physics and Chemistry of Minerals*, 1990, 17: 17–23.
- [22] LIU X, KANZAKI M, XUE X. Crystal structures of  $Zn_2SiO_4$  III and IV synthesized at 6.5–8 GPa and 1273 K [J]. *Physics and Chemistry of Minerals*, 2013, 40: 467–478.
- [23] ITOH S, AZAKAMI T. Thermodynamic studies of ZnO in solids zinc silicate–fundamental studies of zinc extraction by the iron-reduction distillation process (4th report) [J]. *J Min Metall Inst Jpn*, 1989, 105: 685–692.
- [24] LEINENWEBER K, NAVROTSKY A, MCMILLAN P, ITO E. Transition enthalpies and entropies of high pressure zinc metasilicates and zinc metagermanates [J]. *Physics and Chemistry of Minerals*, 1989, 16: 799–808.
- [25] JAK E, LIU N, LEE H G, WU P, PELTON A D, HAYES P. Phase equilibria in the system  $PbO$ – $ZnO$ – $SiO_2$  [C]//Proc 6th Aus IMM Extractive Metallurgy Conference. Brisbane, Victoria Australia: Aus IMM, 1994: 253–255.
- [26] BALE C W, CHATRAN P, DEGTEROV S, ERIKSON G, HACK K, BEN MAHFOUD R, MELANCON J, PELTON A D, PETERSEN P. FactSage thermochemical software and databases [J]. *Calphad*, 2002, 26: 189–228.
- [27] BARIN I. Thermochemical data of pure substances [M]. Weinheim: VCH, 1989.
- [28] KING E G. Heats of formation of crystalline calcium orthosilicate, tricalcium silicate and zinc orthosilicate [J]. *Journal of the American Chemical Society*, 1951, 73: 656–658.
- [29] KITCHENER J A, IGNATOWICZ S. The reduction equilibria of zinc oxide and zinc silicate with hydrogen [J]. *Transactions of the Faraday Society*, 1951, 47: 1278–1286.
- [30] TODD S S. Low-temperature heat capacities and entropies at 298.15 K of crystalline calcium orthosilicate, zinc orthosilicate and tricalcium silicate [J]. *Journal of the American Chemical Society*, 1951, 73: 3277–3278.
- [31] NAVROTSKY A. Thermodynamics of formation of the silicates and germanates of some divalent transition metals and of magnesium [J]. *Journal of Inorganic and Nuclear Chemistry*, 1971, 33: 4035–4050.
- [32] KOZLOVSKA-RÓG A, RÓG G. Thermodynamics of zinc and cobalt silicates [J]. *Polish Journal of Chemistry*, 1979, 53: 2083–2086.
- [33] JAK E, HAYES P. Phase equilibria determination in complex slag systems [J]. *Mineral Processing and Extractive Metallurgy*, 2008, 117: 1–17.
- [34] TANAKA N, ISEKI T, LING L, SHIMPO R, OGAWA O. Standard Gibbs energy of formation of  $Zn_2SiO_4$  [J]. *J Min Metall Inst Jpn*, 1998, 114: 567–572.
- [35] KARAZHANOV S ZH, RAVINDRAN P, VAJEESTON P, ULYASHIN A G, FJELLVÅG H, SVENSSON B G. Phase stability and pressure-induced structural transitions at zero temperature in  $ZnSiO_3$  and  $Zn_2SiO_4$  [J]. *Journal of Physics: Condensed Matter*, 2009, 21: 485801.
- [36] BEKTURGANOV N S, BISSENGALIYEVA M R, GOGOL D B. Calculation of vibrational spectra and thermodynamic functions of a natural zinc silicate–willemite [J]. *Eurasian Chemical Technological Journal*, 2013, 15: 227–232.
- [37] ANDERSSON J O, HELANDER T, HÖGLUND L, SHI P, SUNDMAN B. Thermo-Calc & DICTRA, computational tools for materials science [J]. *Calphad*, 2002, 26: 273–312.
- [38] DAVIES R H, DINSDALE A T, GISBY J A, ROBINSON J A J, MARTIN S M. MTDATA—Thermodynamic and phase equilibrium software from the national physical laboratory [J]. *Calphad*, 2002, 26: 229–271.
- [39] GISBY J A, TASKINEN P, PIHLASALO J, LI Z, TYRER M, PEARCE J, AVARMAA K, BJÖRKLUND P, DAVIES R H, KORPI M, MARTIN S M, PESONEN L, ROBINSON J A J. MTDATA and the prediction of phase equilibria in oxide systems: 30 years of industrial collaboration [J]. *Metallurgical and Materials Transactions B*, 2017, 48: 91–98.
- [40] Scientific Group Thermodata Europe. SGTE database for pure substances, scientific group thermodata [EB/OL] [2018–04–20]. <http://www.sgte.org>.
- [41] BARRY T, DINSDALE A, GISBY J. Predictive thermochemistry and phase equilibria of slags [J]. *JOM*, 1993, 45: 32–38.
- [42] REDLICH O, KISTER A T. Algebraic representation of thermodynamic properties and the classification of solutions [J]. *Industrial and Engineering Chemistry*, 1948, 40: 345–348.
- [43] GALKIN V, KUZNETSOV G, TURKIN A. Thermal expansion of  $ZnSiO_3$  high-pressure phases [J]. *Physics and Chemistry of Minerals*, 2007, 34: 377–381.
- [44] SAUNDERS N, MIODOWNIK A P. CALPHAD calculation of phase diagrams: A comprehensive guide [M]. Oxford: Elsevier Science Ltd., 1998.
- [45] GISBY J, DINSDALE A, BARTON-JONES I, GIBBON A, TASKINEN P. Predicting phase equilibria in oxide and sulphide systems [C]//Proceedings of Sulfide Smelting 2002. Warrendale, PA: TMS, 2002: 533–545.
- [46] LEVIN E M. Liquid immiscibility in oxide systems [C]//Phase Diagrams, Materials Science and Technology. London: Academic Press, 1970: 145–146.
- [47] WEST A R. Solid state chemistry and its applications [M]. Chichester: John Wiley & Sons, 1987.
- [48] SEGNET E R, HOLLAND A E. The system  $MgO$ – $ZnO$ – $SiO_2$  [J]. *Journal of the American Ceramic Society*, 1965, 48: 409–412.

- [49] JAEGER F M, van KLOOSTER H S. Investigations in the field of silicate-chemistry. IV. Some data on the meta- and ortho-silicates of the bivalent metals: Beryllium, magnesium, calcium, strontium, barium, zinc, cadmium and manganese [C]/KNAW Proceedings. Amsterdam, 1916: 896–913.
- [50] TONKOV E U. High pressure phase transformations (Vol. 2) [M]. Moscow: Metallurgiya, 1988: 626.
- [51] FORES A, LLUSAR M, BADENES J A, CALBO J, TENA M A, MONROS G. Cobalt minimization in willemite ( $\text{Co}_x\text{Zn}_{2-x}\text{SiO}_4$ ) ceramic pigments [J]. Green Chemistry, 2000, 2: 93–100.
- [52] BARIN I. Thermochemical data of pure substances [M]. 2nd ed. Weinheim: VCH, 1993.
- [53] KUBASCHEWSKI O, ALCOCK C B. Metallurgical thermochemistry [M]. 5th ed. Oxford: Pergamon Press, 1979.

## ZnO–SiO<sub>2</sub> 体系的热力学评价

Iikka ISOMÄKI<sup>1</sup>, Rui ZHANG<sup>2</sup>, 夏隆巩<sup>3</sup>, Niko HELLSTEN<sup>1</sup>, Pekka A. TASKINEN<sup>1</sup>

1. Thermodynamics and Modelling Research Group, Department of Materials Science and Engineering, School of Chemical Technology, Aalto University, P. O. Box 16200, FI-00076 Aalto, Finland;
2. Department of Materials Science, Royal Institute of Technology, Stockholm 11428, Sweden;
3. 中南大学 冶金与环境学院, 长沙 410083

**摘要:** 含 ZnO 炉渣是贱金属和钢的火法冶金过程中常见的炉渣, 这导致人们对于 ZnO–SiO<sub>2</sub> 体系热力学的兴趣。本文作者对 ZnO–SiO<sub>2</sub> 体系进行全面的文献评述, 对现有实验数据进行批判性评价, 对体系相平衡进行热力学优化, 给出了 ZnO–SiO<sub>2</sub> 体系在  $1.013 \times 10^5$  Pa 总压力下的热力学性质。将熔融氧化物视为缔合溶液, 重新评估了液相的性质。对固体  $\text{Zn}_2\text{SiO}_4$  吉布斯自由能的焓项重新进行拟合, 使之与硅锌矿初晶区的新数据相符。所得热力学数据与新近的实验观测结果吻合良好。这些结果可用于预测热力学性质和相图中的相区, 如液相混溶区的临界点, 预测准确度优于以往的方法。获得了一组优化的模型参数, 在整个组成范围内, 温度从 298 K 到液相线温度, 重新生成了可靠的热力学和相平衡数据, 其误差在实验误差范围内。建立的数据库可用于 Gibbs 自由能最小化软件中热力学性质和有关相图截面的计算。

**关键词:** 热力学评价; ZnO–SiO<sub>2</sub> 体系; 热力学性质; 相图

(Edited by Wei-ping CHEN)